region between 28 and 35°C. The MR of (+) and (−)-$NaBrO_3$ almost agree throughout.

(6) The changes in the properties indicate that some type of a transition in the crystal structure of (+) and (−)-$NaBrO_3$ takes place between 30 and 35°C CGT.

An exact comparison of the present data with the previous measurements is not possible, as the CGT of samples used by the previous workers is not known. However, the following comparisons can be shown. The measured value of the SG (with respect to water at 4°C) for (+) and (−)-$NaBrO_3$ agrees (within 0·5 to 1·2%) with the value of the SG 3·334 (with respect to water at 4°C) reported by Kremers (1857). The SG found here also agrees (within 0·2 to 0·9%) with the value of the SG 3·324, calculated from the unit cell dimension of the $NaBrO_3$ crystal. The RI found in the present investigation for (+) and (−)-$NaBrO_3$, for $\lambda = 5893$ Å, agrees (within 0·013 to 0·075%) with the RI value 1·6165, for $\lambda = 5893$ Å, given by Rose (1910); and agrees (within 0·063%) with 1·6157, for $\lambda = 5893$ Å, found by Poinsot & Mathieu (1955). The magnitudes of the ORP found here for (+) and (−)-$NaBrO_3$, for $\lambda = 5893$ Å, agree (within 0·95 to 3·45%) with the value 2·055 °.mm^{-1}, for $\lambda = 5893$ Å, calculated from the formula for the optical rotatory dispersion given by Kizel, Krasilov & Shamraev (1964).

To make certain that the observed variation of the properties of the crystals is not due to the presence of inclusions, disorder or enantiomorphs in the crystals, the properties were determined for several crystals obtained at the same temperature. The observed properties were found to be reproducible and they vary systematically with the CGT. The optical properties were also found to be reproducible along different directions in the same crystal. Hence, it is concluded that the observed variation of the SG and the optical properties are due to the variation of the CGT. The deviation from Brewster's law was checked for the crystals obtained below 21°C, by performing a converse experiment.

The authors thank the Principal of the Govt. College of Science, Raipur (M.P.), for providing laboratory facilities. One of the authors (Neelkanth Verma) thanks the Vice-Chancellor of Ravishankar University, Raipur (M.P.), for awarding a research fellowship.

References

Chandrasekhar, S. & Madhava, M. S. (1967). *Acta Cryst.* **23**, 911–913.

Craw, J. A. (1896). *Z. Phys. Chem.* **19**, 277. See also Rose (1910), p. 63.

Holden, A. & Singer, P. (1968). *Crystals and Crystal Growing*, pp. 93–107. New York: Doubleday; London: Heinemann; and Bombay: Vakils, Feffer & Simons.

Kizel, V. A., Krasilov, Yu. I. & Shamraev, V. N. (1964). *Opt. Spectrosc.* (*USSR*), **17**, 470–473.

Kremers, P. (1857). *Ann. Phys. Lpz.* **99**, 443. See also Mellor (1946), pp. 330, 331.

Le Blanc, M. & Rohland, P. (1896). *Z. Phys. Chem.* **19**, 261.

Mellor, J. W. (1946) *A Comprehensive Treatise on Inorganic and Theoretical Chemistry*, Vol. 2. London: Longmans.

Poinsot, G. & Mathieu, J. P. (1955). *Ann. Phys.* **12**, 481–486.

Rose, H. (1910). *N. Jahrb. Mineral.* **29**, 53–105.

Traube, H. (1894). *Z. Kristallogr.* **23**, 576. See also Mellor (1946), pp. 330, 331.

Acta Cryst. (1973). B**29**, 7

The Structures of Fluorides. I. Deviations from Ideal Symmetry in the Structure of Crystalline UF_6: A Neutron Diffraction Analysis

By J. C. Taylor, P. W. Wilson and J. W. Kelly

Chemical Technology Division, Australian Atomic Energy Commission Research Establishment, Lucas Heights, Private Mail Bag, Sutherland, New South Wales, Australia

(*Received* 25 *April* 1972; *accepted* 18 *September* 1972)

A neutron-diffraction powder pattern of crystalline UF_6 at 21°C has confirmed the X-ray structure of Hoard & Stroupe [USAEC Report TID-5290 (1958) Paper 45]. From the X-ray data it was not certain whether the fluorine atoms deviated significantly from ideal hexagonal close-packing and the UF_6 octahedra from regularity. The neutron powder pattern of UF_6 was analysed by the profile-fitting method of Rietveld [*Acta Cryst.* (1967), **22**, 151]. Significant deviations from the ideal parameters of Hoard & Stroupe were found. These effects are apparently caused by strong U–U repulsions in the unsymmetrical U^{VI} arrangement and the U–F bonding in the octahedra.

Introduction

An X-ray crystal structure analysis of a single crystal of UF_6 mounted in a capillary was carried out by Hoard & Stroupe (1958) (hereafter H & S) using 60 *hk*0 and 66 *h*0*l* reflexions collected with a Weissenberg camera. The uranium locations were refined by Fourier synthesis, and the fluorine atoms were located in difference syntheses. The crystal data of H & S are given in Table 1 and their atomic coordinates in Table 2.

Table 1. *Crystal data for* UF_6 *at* 21 °C (*Hoard & Stroupe*, 1958)

Orthorhombic: $a=9{\cdot}900$ (2), $b=8{\cdot}962$ (2), $c=5{\cdot}207$ (2) Å, $U=462{\cdot}0$ Å^3, $Z=4$, $D_m=4{\cdot}93$ at 62·5 °C, $D_x=5{\cdot}060$ (5) at 25 °C, M.W. 352·02, $\mu=1200$ cm^{-1} for Cu $K\alpha$.

Space group: *Pnma* (D_{2h}^{16}) or *Pn2a* (C_{2v}^{9}). *Pnma* confirmed by the structure analysis.

Table 2. *Structural parameters in* UF_6 *by neutron powder diffraction compared with the Hoard & Stroupe* (1958) *X-ray and 'ideal' values*

	Coordinate	10^3x	10^3y*	10^3z
U	Neutron	130 (2)	$\frac{1}{4}$	77 (4)
	X-ray	130	$\frac{1}{4}$	81
	Ideal	125	$\frac{1}{4}$	83
F(1)	Neutron	12 (3)	$\frac{1}{4}$	−226 (5)
	X-ray	3	$\frac{1}{4}$	−250
	Ideal	0	$\frac{1}{4}$	−250
F(2)	Neutron	250 (3)	$\frac{1}{4}$	450 (7)
	X-ray	250	$\frac{1}{4}$	417
	Ideal	250	$\frac{1}{4}$	417
F(3)	Neutron	18 (2)	100 (2)	233 (3)
	X-ray	14	93	250
	Ideal	0	83	250
F(4)	Neutron	242 (2)	105 (2)	−73 (6)
	X-ray	246	93	−83
	Ideal	250	83	−83

* Fractional values are not multiplied by 10^3.

The H & S structure is illustrated in Fig. 1 and Fig. 45·3 of their paper. H & S found that the fluorine atoms form a regular, or nearly regular, hexagonal close-packed arrangement, the layers being stacked in the **a** direction. Between the fluorine layers at $x\sim0$, $\frac{1}{4}$, $\frac{1}{2}$ and $\frac{3}{4}$ are four interlayer uranium atoms at the levels $x\sim\frac{1}{8}$, $\frac{3}{8}$, $\frac{5}{8}$ and $\frac{7}{8}$. One sixth of the available octahedral holes are occupied by uranium atoms.

H & S noted that the area of the *bc* face was consistent with an orthogonal unit of six spheres of diameter 3·0 Å in hexagonal close-packing. The orthorhombic cell was such that the *b* dimension (8·96 Å) corresponded to three diameters and the *c* dimension (5·21 Å) to the orthogonal repeat $3\sqrt{3}=5{\cdot}20$ Å. They also noted that the *a* repeat distance of 9·90 Å corresponded to a four-layer sequence in hexagonal close-packing of spheres of diameter 3·0 Å (theoretical repeat = 9·80 Å). They calculated 'ideal' coordinates for this h.c.p. fluorine arrangement, which are shown in Table 2, and in this ideal structure, all F–F contacts were 3·0 Å. The symmetry was reduced to orthorhombic by inclusion of the uranium atom in the ideal positions ($\frac{1}{8}$, $\frac{1}{4}$, $\frac{1}{12}$) *etc.*, giving regular UF_6 octahedra with U–F distances of 2·12 Å. H & S were not certain whether their coordinates differed significantly from the ideal arrangement.

It appeared to us that the structure of crystalline UF_6 should deviate from this 'ideal' arrangement for the following reasons:

(i) The fluorine layers should be distorted by U–F bonding in the localized octahedra.

(ii) The uranium arrangement in the crystal is unsymmetrical and the U^{VI} atoms highly charged; thus

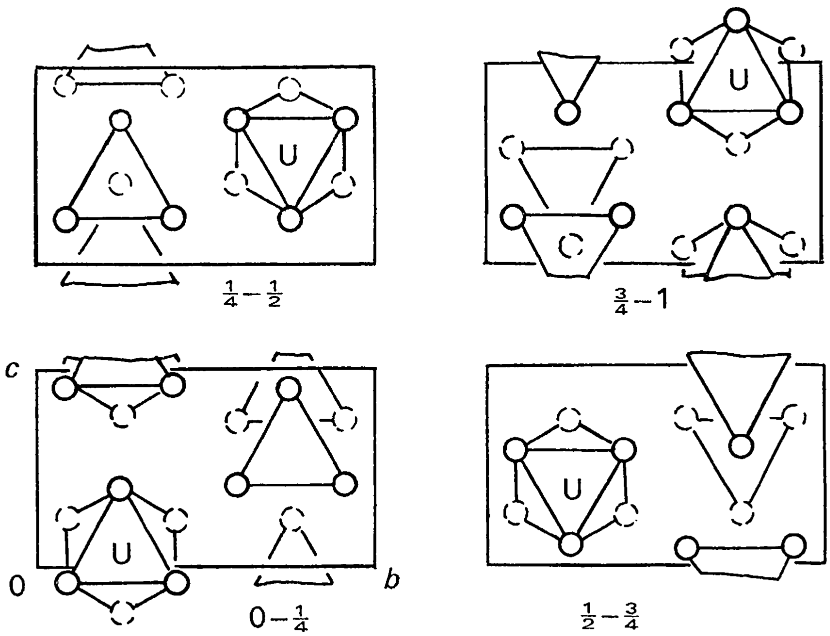

Fig. 1. The structure of UF_6 according to Hoard & Stroupe (1958). Each diagram gives the atomic arrangement in a layer of thickness *a*/4.

the ideal arrangement should be disturbed by U–U repulsions.

(iii) The Pauling (1960) diameter of a fluoride ion is 2·70 Å, lower than the contact distance of 3·0 Å assumed by H & S. Because of the highly reactive nature of UF_6 and its large crystal vapour pressure at 21 °C, preliminary attempts to contain and keep large single crystals for neutron diffraction were unsuccessful. A neutron powder pattern of satisfactory appearance was, however, obtained, and this was used in an attempt to confirm the H & S structure and determine whether significant deviations from the ideal structure of H & S were present.

Experimental

Uranium hexafluoride crystals were prepared by direct fluorination of UO_2. Hydrogen fluoride was removed by absorption into sodium fluoride, and the UF_6 was purified by a double sublimation. The UF_6 crystals, approximately 0·5 mm in diameter, were placed in a thin-walled Kel–F tube of diameter 1·5 cm. The crystals were roughly spherical with irregular faces, and it was considered that preferred orientation would not be significant; hence no efforts were made to further randomize the crystals. A room-temperature neutron-diffraction powder pattern was collected on the AAEC double crystal neutron spectrometer on the research reactor HIFAR. The pattern was collected to $2\theta = 45°$ ($\sin\theta/\lambda = 0{\cdot}35$), with $\lambda = 1{\cdot}076$ Å. The double-crystal method (Caglioti, 1970) was used, and this resulted in sharp maxima and good peak-to-background ratios. A blank run with the Kel–F tube gave a peak at 11·4° 2θ, and no other maxima. The data below $2\theta = 13°$ were therefore rejected from the analysis. No absorption corrections were necessary.

Analysis of the data

The powder diffraction pattern of UF_6 was analysed by the profile-fitting method of Rietveld (1967), in which the component peaks are assumed to be Gaussians and each count along the scan is treated as a single observation. This was readily achieved by modifying the crystallographic least-squares program *ORFLS* (Busing, Martin & Levy, 1962).

A least-squares refinement of the cell constants was carried out with the neutron data, with a view to ac-

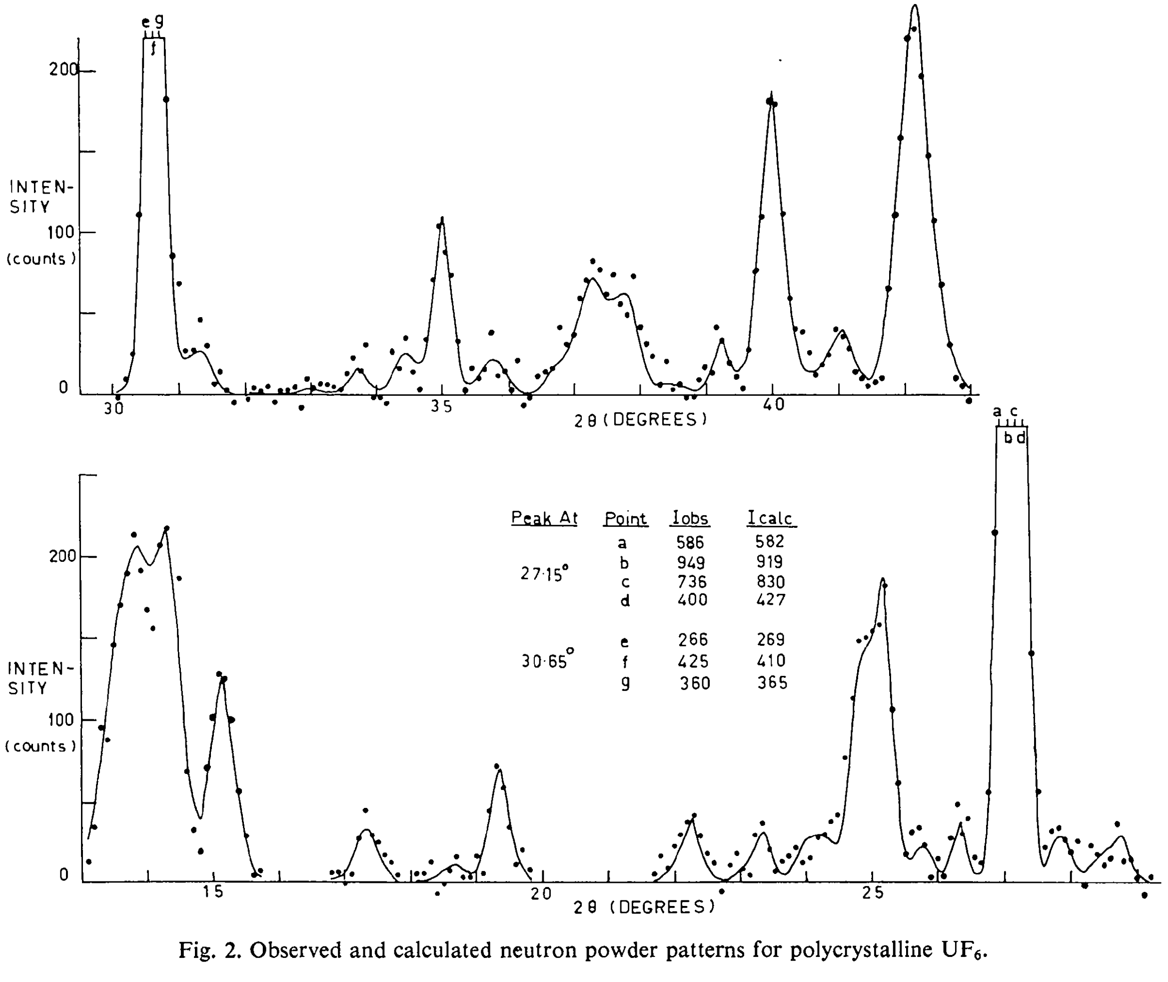

Peak At	Point	Iobs	Icalc
27·15°	a	586	582
	b	949	919
	c	736	830
	d	400	427
30·65°	e	266	269
	f	425	410
	g	360	365

Fig. 2. Observed and calculated neutron powder patterns for polycrystalline UF_6.

curately locating the positions of the component *hkl* reflexions; these constants were identical to those of H & S within the errors, which were larger with the neutron powder data. The *ORFLS* input was a list of the intensities corrected for background, $(I-B)$, with their e.s.d.'s to give least-squares weighting factors $w=[\sigma^2(I-B)]^{-1}$. The *hkl* contributing at each data point were computed along with their Gaussian factors, and a total of 987 *hkl* reflexion cards were generated, after systematic absences were eliminated. The required intermediate sums were computed in *ORFLS* corresponding to the superposition of data, and the correct number of observations, NO (the number of data points which were contributed to by one or more *hkl* reflexions = 260) was used in the computation where required. The neutron scattering lengths used were those of the Neutron Diffraction Commission (1969). An overall isotropic temperature factor B was used, and refined to 3·1 (2) Å². The final standard deviation of an observation of unit weight, $[\sum w(I_o-I_c)^2/(\text{NO}-\text{NV})]^{1/2}$, where NV is the number of variables, was 0·9. The parameters resulting from the profile analysis are given in Table 2, and the interatomic distances and and angles in Table 3.

Table 3. *Interatomic distances and angles in* UF_6 *by neutron powder diffraction in* Å *and degrees*

In octahedron

U—F(1)	1·96 (3)	F(3)–U–F(4)	91·7 (8) (2×)
U—F(2)	2·28 (4)	F(3)–U–F(1)	89·7 (10) (2×)
U—F(3)	1·92 (2) (2×)	F(3)–U–F(2)	86·5 (10) (2×)
U—F(4)	1·88 (2) (2×)	F(3)–U–F(3)	88·6 (15)
F(3)–F(3)	2·69 (4)	F(4)–U–F(4)	88·0 (17)
F(2)–F(3)	2·89 (3) (2×)	F(4)–U–F(1)	91·0 (12) (2×)
F(1)–F(3)	2·74 (3) (2×)	F(4)–U–F(2)	92·9 (11) (2×)
F(3)–F(4)	2·73 (3) (2×)	F(2)–U–F(1)	174·7 (17)
F(4)–F(4)	2·60 (4)	F(4)–U–F(3)	179·3 (14) (2×)
F(2)–F(4)	3·02 (3) (2×)		
F(1)–F(4)	2·74 (3) (2×)		

Other F–F contacts

Intralayer		Interlayer	
F(1)–F(3)	3·12 (3)	F(4)–F(3)	3·26 (3)
F(1)–F(3)	3·15 (2)	F(4)–F(1)	3·16 (3)
F(3)–F(3)	3·04 (4)	F(4)–F(3)	3·26 (3)
F(3)–F(3)	3·33 (3)	F(4)–F(3)	3·17 (2)
F(2)–F(4)	3·18 (2)	F(3)–F(2)	3·13 (3)
F(2)–F(4)	2·80 (3)	F(2)–F(1)	2·97 (3)
F(4)–F(4)	3·21 (2)	F(2)–F(1)	2·89 (4)

U–U separations

In mirror plane	Between mirror planes
5·27 (1), 5·21 (1), 6·01 (2)	5·70 (1), 5·23 (2), 6·79 (3)

The observed and calculated neutron diffraction patterns are compared in Fig. 2.

Discussion

The neutron parameters, compared with the ideal and X-ray parameters

The neutron parameters are compared with the ideal parameters in Table 4. To assess the significance of the deviations from the ideal positions, the quantities Δ/σ, where Δ is the difference between a neutron and ideal parameter and σ is the standard deviation of the neutron parameter, were calculated. The Δ/σ values in Table 4 range from 0·0 to 11·0. Taking a Δ/σ value of 4 or greater as representing a significant departure from an ideal coordinate, Table 4 shows that 8 of the 12 positional parameters differ significantly from the ideal positions of H & S. Comparing the neutron coordinates with the X-ray coordinates in Table 3, it can be seen that the deviations from the ideal positions in the x and z parameters are all in the same directions as the X-ray deviations, the neutron deviations being all larger [except for x (U)]. H & S quoted ideal coordinates only for the z coordinates as the accuracy of their z coordinates was lower because of the lower index range; the neutron z parameters, however, indicate departures from the ideal coordinates (the z parameters

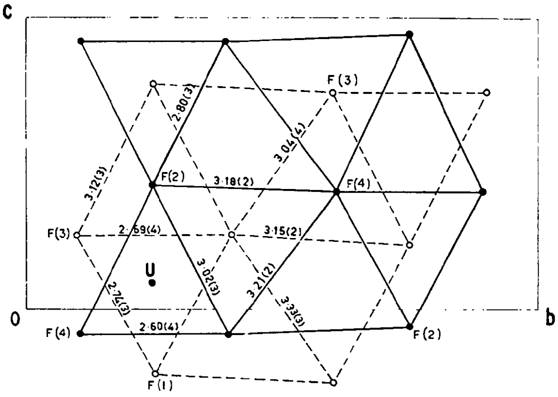

Fig. 3. The fluorine layers at $x\sim 0$ (open circles) and $x\sim\frac{1}{4}$ (full circles). The radii correspond to the r.m.s. radial positional errors.

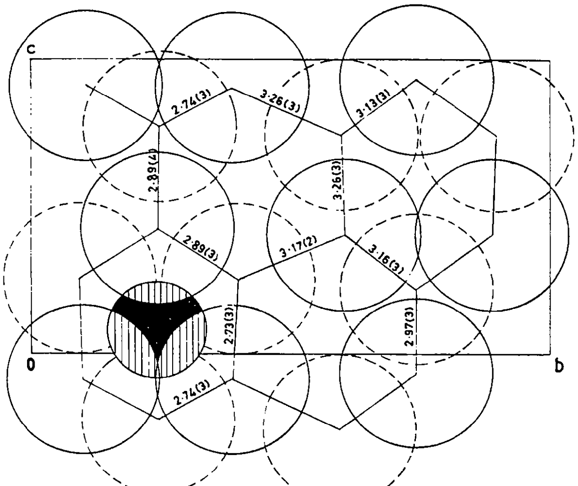

Fig. 4. The fluorine layers at $x\sim 0$ and $x\sim\frac{1}{4}$, showing interlayer contacts. Radii of circles correspond to ionic radii for F^- and U^{6+}.

are also less accurate than the x and y parameters in the present analysis).

Table 4. *Comparison of the ideal and neutron parameters (as listed in Table 2). The quantities Δ are the differences between corresponding ideal and neutron parameters in* Å, *and the σ values are the neutron standard deviations in* Å

	Parameter	$\|\Delta\|$(Å)	$\|\Delta\|/\sigma$
U	x	0·050 (20)	2·5
	z	0·031 (21)	1·5
F(1)	x	0·120 (30)	4·0
	z	0·125 (26)	4·8
F(2)	x	0·000 (30)	0·0
	z	0·172 (36)	4·8
F(3)	x	0·180 (20)	9·0
	y	0·153 (18)	8·5
	z	0·088 (16)	5·5
F(4)	x	0·080 (20)	4·0
	y	0·198 (18)	11·0
	z	0·052 (31)	1·7

H & S were not sure whether their parameters deviated significantly from the ideal coordinates; the present analysis, however, clearly shows significant deviations from the ideal positions, which are, in the case of the x and y parameters, in the same direction as the X-ray deviations.

The fluorine layers

The F–F distances in Table 3 lie between 2·60 (4) and 3·33 (3) Å. The short F–F distances occur in the UF_6 octahedra, while the F–F distances bridging the octahedra are longer. The fluorine atoms cluster around the U^{VI} atoms and thus distort the fluorine layers from perfect h.c.p. symmetry.

Fig. 3 shows the fluorine layers at $x \sim 0$ (open circles) and $x \sim \frac{1}{4}$ (dark circles) and the uranium atom midway between the layers at $x \sim \frac{1}{8}$, together with the intralayer F–F contacts. The radii of the circles representing the atoms correspond to the r.m.s. radial positional errors. The deviations of the fluorine layers from ideal hexagonal symmetry can be seen. The structure of UF_6 tends to be layered in the mirror planes because of the U–F bonding in the octahedra. The clustering of the fluorine atoms around the uranium atoms can also be seen in Fig. 4, which illustrates the interlayer contacts. In Fig. 4 circles at the atomic positions correspond to the ionic diameters, which are taken as 1·7 Å for U^{6+} (Zachariasen, 1950) and 1·35 Å for F^-. Again short approaches occur across the mirror planes, and long approaches between them.

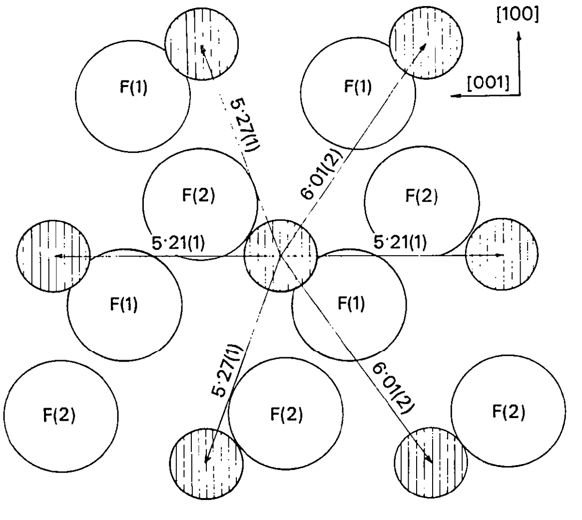

Fig. 5. The atomic arrangement in UF_6 in the mirror plane at $y=\frac{1}{4}$.

The UF_6 *octahedron*

The F–F edges of the UF_6 octahedron lie between 2·60 (4) and 3·02 (3) Å, and the F–U–F angles between 86·5 (10) and 92·9 (11)° (Table 3). The octahedron appears to be flattened in a direction perpendicular to the mirror plane since the F(3)–F(3) and F(4)–F(4) distances across the plane are shorter than the other F–F distances in the octahedron. The F–F contact distances are normal, and the F–U–F 'diameters' nearly linear.

There appear to be differences in the U–F bond lengths in the octahedron (Table 3). Two U–F(3) distances of 1·92 (2) Å and two U–F(4) distances of 1·88 (2) Å occur. Nearly normal to the F(3) F(3) F(4) F(4) plane are one U–F(1) bond of length 1·96 (3) Å and one U–F(2) bond of length 2·28 (4) Å. Although the latter bond has a considerable z component, an off-centre displacement of the uranium atom in the octahedron is likely when the effect of U–U repulsions is considered.

The uranium arrangement is not highly symmetrical, as can be seen from the U–U distances in Table 3. The important U–U interactions in this case are those in the mirror planes, as the effects of the other interactions across the mirror planes cancel. The atoms lying in the mirror plane are shown in Fig. 5. The central uranium atom is not in the centre of the rectangle formed by the two upper and two lower uranium atoms. There is a shorter U–U vector of 5·27 (1) Å and a longer U–U vector of 6·01 (2) Å (the vectors of 5·21 Å cancel). The shorter U–U interaction of 5·27 Å should be very strong, as there is little intervention by fluorine atoms, whereas the vector of 6·01 Å is screened by intervening F(1) atoms. To relieve the strain caused by the stronger U–U interaction, an off-centre displacement of the central U atom in the direction of $-\mathbf{c}$ would be expected, *i.e.* the U–F(2) distance would be expected to be longer than U–F(1). Distortions from ideal symmetry in the UF_8 coordination polyhedron in Rb_2UF_6 (Kruse, 1971) have also been ascribed to the effect of unsymmetrical U–U repulsions.

Off-centre positions for cations in octahedra are commonly encountered in ferroelectrics and other metal oxide structures. Megaw (1968*a*) has explained the off-centring as the result of relaxation of tensions in the octahedra caused by anion–anion repulsions while Orgel (1959) considers the displacements to be a result of decreasing stability of the octahedral structure with decreasing cation size, with a consequent tendency to form fivefold and, finally, tetrahedral coordination. In the alkali metal niobates (Megaw, 1968*b*) cations are displaced by as much as 0·26 Å. These mechanisms may also be contributing to the distortion of the UF_6 octahedron.

We wish to thank Dr G. W. Cox for programming assistance.

References

Busing, W. R., Martin, K. O. & Levy, H. A. (1962). *ORFLS*. Report ORNL-TM-305. Oak Ridge National Laboratory, Oak Ridge, Tennessee.

Caglioti, G. (1970). *Thermal Neutron Diffraction*. Edited by B. T. M. Willis, Chap. 2. Oxford Univ. Press.

Hoard, J. L. & Stroupe, J. D. (1958). U.S.A.E.C. Report TID-5290, Paper 45.

Kruse, F. H. (1971). *J. Inorg. Nucl. Chem.* **33**, 1625–1627.

Megaw, H. D. (1968*a*). *Acta Cryst.* B**24**, 149–153.

Megaw, H. D. (1968*b*). *Acta Cryst.* A**24**, 589–604.

Neutron Diffraction Commission (1969). *Acta Cryst.* A**25**, 391–392.

Orgel, L. E. (1958). *Faraday Soc. Discuss.* **26**, 138–144.

Pauling, L. (1960). *The Nature of the Chemical Bond*, 3rd ed. Ithaca: Cornell Univ. Press.

Rietveld, H. M. (1967). *Acta Cryst.* **22**, 151–152.

Zachariasen, W. H. (1950). *Struct. Rep.* **13**, 435.

Acta Cryst. (1973). B**29**, 12

The Crystal and Molecular Structure of Di-μ-hydroxobis[di(1,10-phenanthroline)chromium(III)] Chloride Hexahydrate

By Jack T. Veal,[*] William E. Hatfield and Derek J. Hodgson[†]

Department of Chemistry, University of North Carolina, Chapel Hill, North Carolina 27514, *U.S.A.*

(*Received* 17 *May* 1972; *accepted* 14 *September* 1972)

The crystal and molecular structure of di-μ-hydroxobis[di(1,10-phenanthroline)chromium(III)] chloride hexahydrate, $[Cr(phen)_2OH]_2Cl_4.6H_2O$, has been determined from three-dimensional counter X-ray data. The material crystallizes in the triclinic space group $P\bar{1}$ with two dimeric formula units in a cell whose dimensions are $a=14·056$ (7), $b=11·296$ (6), $c=18·990$ (9) Å, $\alpha=87·15$ (3), $\beta=107·63$ (2), and $\gamma=74·68$ (3)°. The observed and calculated densities are 1·39 (4) and 1·342 g cm^{-3} respectively. The structure has been refined by full-matrix least-squares techniques to a conventional R value of 0·077 for 3392 independent intensities greater than three times their estimated standard deviations. The complex consists of pairs of chromium atoms which are linked by two hydroxo bridges, with two 1,10-phenanthroline groups coordinated to each metal; the coordination geometry around each chromium is roughly octahedral. The average Cr–N and Cr–O bond lengths are 2·052 (6) and 1·927 (6) Å respectively, while the Cr–Cr separation is 3·008 (3) Å and the average Cr–O–Cr angle is 102·7 (4)°. The geometry of this complex is compared with that of $[Cr(gly)_2OH]_2$ and with those of complexes of the type $[CuLOH]_2^{n+}$, and the magnetic properties of the complex are discussed in terms of the bridging geometry.

Introduction

We have recently been interested in attempting to correlate the structural and magnetic properties of magnetically condensed copper(II) and chromium(III) systems, with especial emphasis on hydroxo- and halogen-bridged dimeric species (Hodgson, Hale & Hatfield, 1971; Meyer, Singh, Hatfield & Hodgson, 1972; Hodgson, Veal, Hatfield, Jeter & Hempel, 1972). From our magnetic and structural investigations of the complex $[Cu(EAEP)OH]_2^{2+}$, where EAEP is the bidentate ligand 2-(2-ethylaminoethyl)pyridine (Lewis, Hatfield & Hodgson, 1972; Jeter, Lewis, Hempel, Hodgson & Hatfield, 1972) and similar studies on the analogous systems $[Cu(bipy)OH]_2^{2+}$, where bipy is 2,2′-bipyridine (Casey, Hoskins & Whillans, 1970; Majeste & Meyers, 1970; Barnes, Hodgson & Hatfield, 1972) and $[Cu(tmen)OH]_2^{2+}$, where tmen = tetramethylethylenediamine (Mitchell, Bernard & Wasson, 1970; Cole & Brumage, 1970) we were able to deduce that the value of $2J$, the singlet–triplet energy separation, decreases as the Cu–O–Cu bridging angle φ increases, and that $2J$ changes from positive to negative in the region 97 to 99° (Lewis *et al.*, 1972).

We have recently extended these studies to chromium(III) complexes of the type $[CrL_2(OH)]_2^{n+}$, where L is a bidentate ligand, and recently reported the structural and magnetic characterization of $[Cr(gly)_2OH]_2$,

---

[*] Tennessee Eastman Corporation Fellow, 1971–72.

[†] Author to whom correspondence should be addressed.